

AD-A051 504

ROCKWELL INTERNATIONAL THOUSAND OAKS CALIF SCIENCE --ETC F/G 7/2  
HETEROGENEOUS DECOMPOSITION OF OZONE ON SULFURIC ACID SURFACES --ETC(U)  
SEP 77 A B HARKER

DOT-TSC-1202

UNCLASSIFIED

SC5078.18FR

FAA-AEQ-77-12

NL

1 of 1  
AD  
A051504



END

DATE

FILMED

4-78

DDC

Report No. FAA-AEQ-77-12

(12)

HETEROGENEOUS DECOMPOSITION OF OZONE ON SULFURIC  
ACID SURFACES AT STRATOSPHERIC TEMPERATURES

SC

Alan B. Harker  
Science Center  
Rockwell International  
1049 Camino Dos Rios  
Thousand Oaks, CA. 91360



SEPTEMBER 1977

FINAL REPORT

Document is available to the U.S. public through the  
National Technical Information Service,  
Springfield, Virginia 22161

Prepared for

U.S. DEPARTMENT OF TRANSPORTATION  
FEDERAL AVIATION ADMINISTRATION  
Washington, D. C. 20590

D D C  
RECORDED  
MAR 20 1978  
REGULAR B  
J

This document is disseminated under sponsorship of the Department of Transportation in the interest of information exchange. The Government assumes no liability for its contents or use thereof.

The work reported in this document was conducted under contract No. DOT-TSC-1202 for the High Altitude Pollution Program, Office of Environmental Quality, Federal Aviation Administration, U.S. Department of Transportation. The publication of this report does not indicate endorsement by the Federal Aviation Administration or the Department of Transportation, nor should the contents be construed as reflecting the official position of either agency.

## Technical Report Documentation Page

18. Report No. <b>19</b> FAA-AEQ-77-12	2. Government Accession No.	3. Recipient's Catalog No. <b>9</b> Final rept. 28 Jun 76	
4. Title and Subtitle <b>HETEROGENEOUS DECOMPOSITION OF OZONE ON SULFURIC ACID SURFACES AT STRATOSPHERIC TEMPERATURES</b>		5. Report Date <b>27 Jun 77</b> Sept 1977	
6. Author(s) <b>B. Harker</b>		7. Author(s) <b>Alan</b>	
8. Performing Organization Report No. <b>14</b> SC5078.18FR		9. Performing Organization Name and Address Rockwell International Science Center 1049 Camino Dos Rios Thousand Oaks, CA. 91360	
10. Work ID No. (TRAIL) <b>12/32p</b>		11. Contract or Grant No. <b>15</b> DOT-TSC-1202	
12. Sponsoring Agency Name and Address U. S. Department of Transportation Federal Aviation Administration Systems Research and Development Service Washington DC 20590		13. Type of Report and Period Covered Final Report 6/28/76 thru 6/27/77	
14. Sponsoring Agency Code FAA/AEQ-10			
15. Supplementary Notes			
16. Abstract Methods of forming sulfuric acid aerosols at stratospheric temperatures were investigated, and the rate constant for the heterogeneous decomposition of ozone on sulfuric acid surfaces was determined over the temperature range 217 to 263K. The dependence of the decomposition rate constant on ozone concentration, relative humidity, and sulfuric acid surface area were studied and the data was interpreted in terms of the heterogeneous gas-surface kinetic model proposed by Judeikis and Siegel (1973). The role of heterogeneous reactions in the stratosphere is discussed, and recommendations for further experimental work are presented. The measured ozone first order decay efficiencies were found to obey the empirical relationships $\gamma = [5.85 \times 10^5 \exp(1081/T)]^{-1}$ and $\gamma = [3.06 \times 10^4 \exp(-2360/T)]^{-1}$ reaction/collision on $\text{H}_2\text{SO}_4$ and 0.045 mole fraction $\text{H}_2\text{SO}_4$ in $\text{H}_2\text{O}$ respectively for T between 217-263K.			
17. Key Words heterogeneous ozone decomposition stratosphere stratospheric aerosols $\text{H}_2\text{SO}_4$ aerosol generation	18. Distribution Statement Document is available to the U.S. public through the National Technical Information Service, Springfield, Virginia 22161.		
19. Security Classif. (of this report) Unclassified	20. Security Classif. (of this page) Unclassified	21. No. of Pages 27	22. Price

## PREFACE

This report summarizes the results of an experimental effort to generate sulfuric acid aerosols at stratospheric temperatures, and to determine the rate coefficients for the heterogeneous decay of ozone on sulfuric acid surfaces over the temperature range 200 - 250K. This study was sponsored by the High Altitude Pollution Program of the Federal Aviation Agency in the Department of Transportation.

## Participants

A. B. Harker  
W. W. Ho  
J. J. Ratto

ACCESSION for	
NTIS	White Section <input checked="" type="checkbox"/>
DDC	Buff Section <input type="checkbox"/>
UNANNOUNCED <input type="checkbox"/>	
JUSTIFICATION _____	
-----	
BY _____	
DISTRIBUTION/AVAILABILITY CODES	
Dist.	AVAIL. 200 or SPECIAL
A	

## TABLE OF CONTENTS

	Page
1.0 INTRODUCTION	1
2.0 EXPERIMENTAL TECHNIQUE AND APPARATUS	3
3.0 DATA ANALYSIS AND RESULTS	10
4.0 DISCUSSION	22
5.0 RECOMMENDATIONS FOR FUTURE RESEARCH	25
REFERENCES	27

## LIST OF FIGURES

Figure 1	SCHEMATIC DIAGRAM OF REFRIGERATED REACTION CHAMBER	4
Figure 2	SCHEMATIC DIAGRAM OF INFRARED SPECTROSCOPIC SYSTEM USED TO MONITOR OZONE ABSORPTION IN REACTION CELL	5
Figure 3	SCHEMATIC DIAGRAM OF SHEATHED FLOW AEROSOL PRE- COOLING SYSTEM	7
Figure 4	LOG-NORMAL PLOT OF NUMBER CONCENTRATION OF H <sub>2</sub> O AND H <sub>2</sub> SO <sub>4</sub> AEROSOLS GENERATED IN FLOW EXPERIMENTS.	12
Figure 5	LOG-NORMAL PLOT OF SURFACE AREA CONCENTRATION OF H <sub>2</sub> O AND H <sub>2</sub> SO <sub>3</sub> AEROSOLS GENERATED IN FLOW EXPERIMENTS.	13
Figure 6	SEMI-LOGARITHMIC PLOT OF THE OPTICAL DENSITY OF THE 9.6 MICRON OZONE OPTICAL DENSITY VERSUS TIME FOR THREE STATIC CELL REACTION EXPERIMENTS. THE DATA HAVE BEEN NORMALIZED TO THE SAME INITIAL OPTICAL DENSITY OF OZONE AND TO THE SAME SURFACE AREA OF H <sub>2</sub> SO <sub>4</sub> .	18
Figure 7	SEMI-LOGARITHMIC PLOT OF THE MEASURED REACTION EF- FICIENCY (REACTIONS/COLLISION) OF THE OZONE DECOMPOSITION VERSUS RECIPROCAL ABSOLUTE TEMPERATURE FOR FUMING H <sub>2</sub> SO <sub>4</sub> AND DILUTE H <sub>2</sub> SO <sub>4</sub> IN H <sub>2</sub> O.	19

HETEROGENEOUS DECOMPOSITION OF OZONE ON SULFURIC  
ACID SURFACES AT STRATOSPHERIC TEMPERATURES

BY

Alan B. Harker  
Member of Technical Staff  
Rockwell International Corporation

1.0 INTRODUCTION

The catalytic removal of stratospheric ozone by oxides of nitrogen and chlorine associated with the chemical reactions of emissions from high-flying aircraft and rockets as well as the vertical diffusion of ground level pollutants has received considerable attention from the scientific community. The concern has been centered around the potential for harmful effects to mankind and other life as the decrease in stratospheric ozone allows more ultraviolet radiation to reach the earth's surface.(1) Of secondary concern has been the possibility of climatic change due to the formation of stratospheric aerosols from the gas-phase oxidation of the sulfur dioxide from propulsion effluents and volcanic activities to form sulfuric acid.(2) Primary attention in most stratospheric research has been given to developing mathematical chemistry and transport models and measuring the parameters required to allow the prediction of the chemical cycles involved in the upper atmosphere. The chemical reactions considered in these models have almost exclusively been homogeneous gas phase reactions, although as pointed out by Cadle et al (3) and Judeikis (4) heterogeneous gas-surface reactions with stratospheric particles could play a significant role in the chemistry of some trace gas species. Their argument is based on the fact that the particle concentration in the lower stratosphere is large enough that collisions of air molecules with the particle surfaces is relatively rapid. Cadle calculates that at twenty km altitude a gas molecule spends on the average  $10^4$  seconds before colliding with an aerosol particle.

For stratospheric trace gases whose destruction time by homogeneous reactions is quite slow and which are removed mainly by transport to the troposphere, typical lower stratospheric residence times are on the order of  $10^7$ - $10^8$  seconds. If such gases were to react on particle surfaces as often as once in every  $10^4$  collisions, these heterogeneous reactions would provide a significant

"sink". Some trace gases for which such heterogeneous reactions have the potential for importance include  $\text{HNO}_3$ ,  $\text{ClNO}_3$ ,  $\text{N}_2\text{O}_5$  and  $\text{O}_3$ .

The stratospheric particles on which heterogeneous reactions would occur have been found to be made up primarily of sulfate in the form of super-cooled or frozen sulfuric acid and crystalline ammonium sulfate, with trace amounts of silicon, chlorine, bromine, and sodium. (2) There may also be small quantities of metal elements such as Al, Fe, and V in the particles from propulsion effluents. It is postulated that stratospheric aerosols are formed by the photochemical oxidation of gaseous  $\text{SO}_2$  to form sulfuric acid which nucleates either homogeneously or heterogeneously to form aerosol particles. Hence the measurement of the catalytic properties of sulfuric acid particle surfaces towards chemical reactions of stratospheric gases is one of the principal requirements for assessing the importance of heterogeneous reactions in the upper atmosphere.

The goal of this study was to generate sulfuric acid particles at stratospheric temperatures and to study the kinetics of the heterogeneous reaction of ozone with the sulfuric acid surface. During the course of the study sulfuric acid aerosols were reacted at stratospheric temperatures in a flow stream with ozone. These experiments showed the heterogeneous reaction of  $\text{O}_3$  with the particle surfaces to have an efficiency of less than  $10^{-6}$  reactions per gas-surface collision. To obtain a more accurate measure of the reaction rate static cell experiments were carried out with ozone exposed to a known surface area of sulfuric acid and sulfuric acid in water over the temperature range 217-263K.

## 2.0 EXPERIMENTAL TECHNIQUE AND APPARATUS

The experimental apparatus constructed during the course of this study was designed with the intention of providing a chamber with a minimum of surface area to volume in which flow experiments could be conducted with a mixture of aerosols and reactant gases over a temperature range from 210 to 290K. The reaction chamber was also designed to provide both gas and particle sampling and analysis equipment to characterize the progress of the chemical reaction. The details of the apparatus are described in the following discussion.

### Reaction Chamber

The reaction chamber was constructed from a 122 cm long, 15.2 cm inner diameter Corning Pyrex glass pipe. The end of the pipe was adapted for o-ring fittings and aluminum end plates were attached to it with viton o-ring seals. As shown in Figure 1, the chamber was mounted in an insulating box constructed of 5 cm thick styrafoam lined with Teflon sheeting and fiberglassed for rigidity. To provide cooling a NESLAB LT-9 refrigeration unit was connected to the system by means of copper cooling coils, wrapped around the reaction chamber. By pumping methanol through the cooling coils the LT-9 unit was capable of cooling the chamber to temperatures between 210 and 290 K with a thermal stability of  $\pm 1$  degree over a 90 hour period.

The end plates of the chamber were machined to accept 2.5 cm IRTRAN infrared optical windows, an alcohol thermometer, and both gas and aerosol inlet and sampling ports. As shown in the schematic, the aerosol sampling ports were arranged to provide analysis samples along the center line of the reaction chamber with a minimum of sample loss on the walls of the sampling tubes. The ability to move the sampling probe back and forth through the system allowed the uniformity of the aerosol concentration and size distribution to be observed.

### Infrared Spectroscopic System

The infrared spectroscopic system was set up in a two detector mode, such that  $I$  and  $I_0$  measurements could be made simultaneously. The system shown in Figure 2 had a Nernst Glower source which was chopped at 246 Hz by a mechanical chopper to produce an AC signal. A portion of the chopped signal was passed through a 0.62 micron longwave length pass filter and onto the infrared sensitive photoresistor to provide a continuous measurement of the Nernst Glower intensity. The main portion of the infrared beam was passed through the reaction chamber, onto a collection mirror assembly, through a 1/4 meter Jerral Ash monochromater,

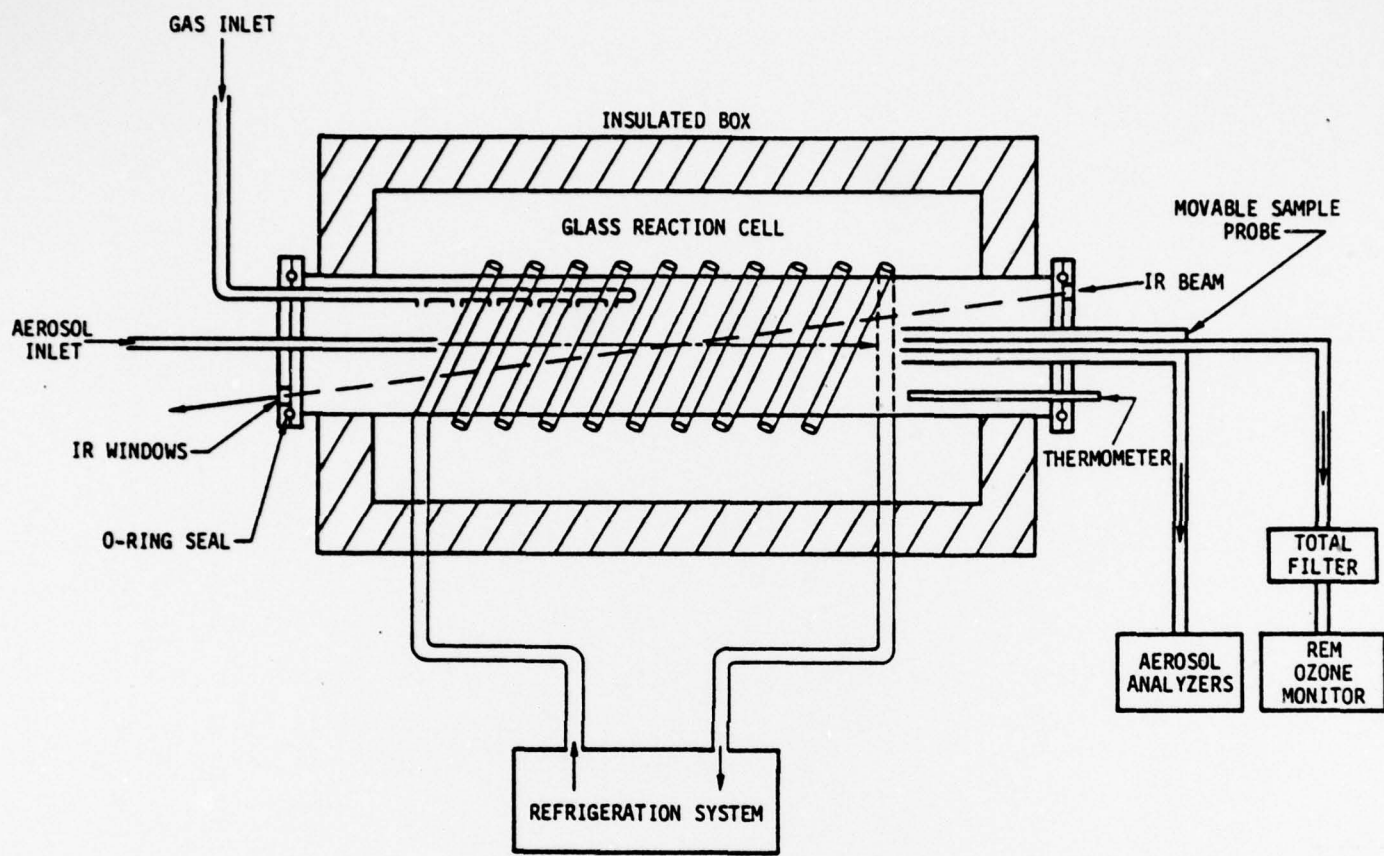


Figure 1. Schematic Diagram of Refrigerated Reaction Chamber

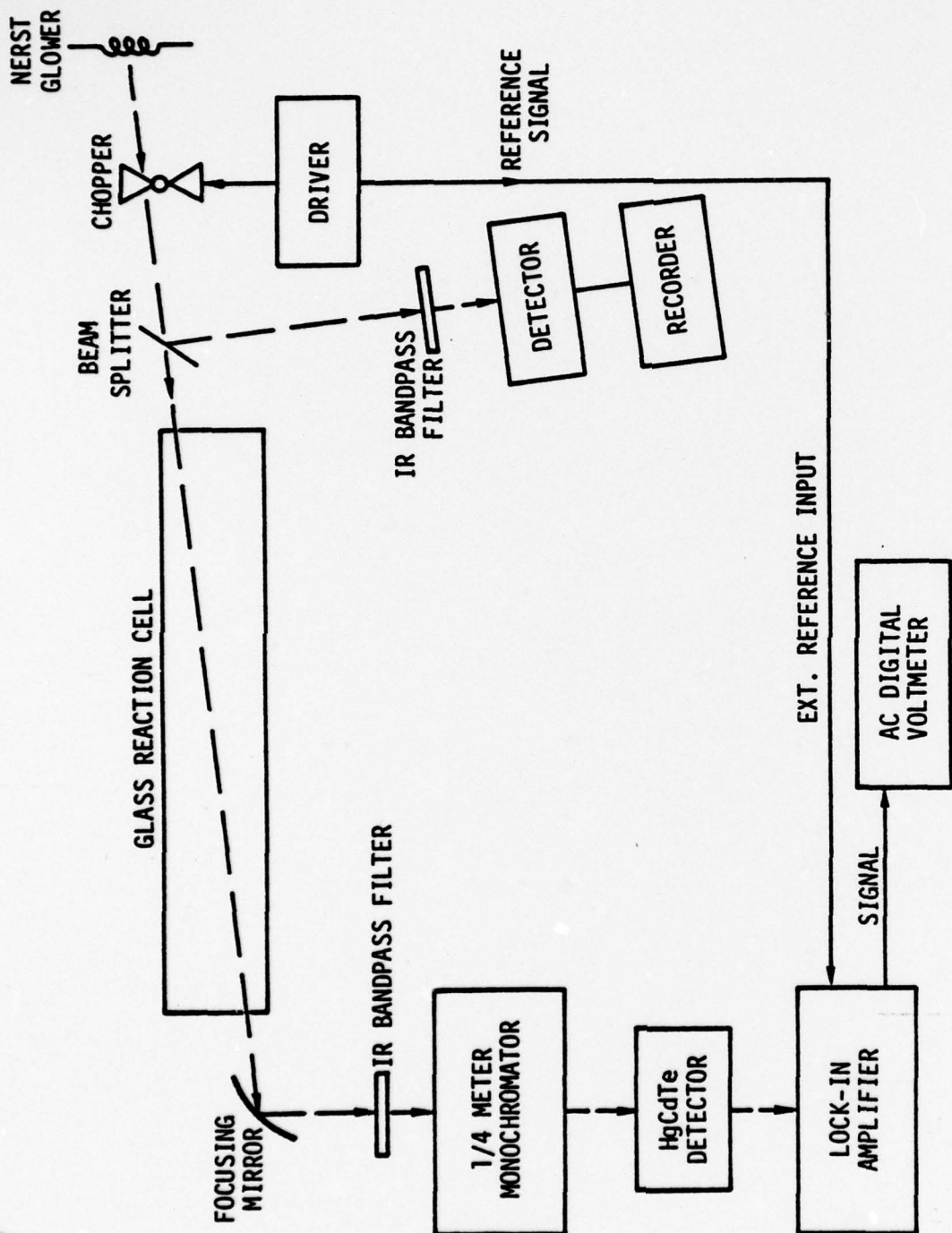


Figure 2. Schematic Diagram of Infrared Spectroscopic System used to Monitor Ozone Absorption in Reaction Cell

and onto a liquid nitrogen cooled HgCdTe photodetector. The HgCdTe detector had its peak sensitivity at 10 microns, and the monochromator was equipped with a 50 groove/mm, 10 micron blaze grating with an order sorting filter on the entrance slit. This combination provided maximum sensitivity to the strong ozone absorption at 9.6 microns. The 246 Hz signal from the reference detector was continuously monitored by an AC voltmeter, and the output from the HgCdTe detector was synchronously rectified by a lock-in amplifier and the resulting signal intensity displayed on a digital voltmeter. The output of the two detectors were calibrated against each other over the full range of light intensities utilized in this study to provide quantitative absorption measurements.

#### Aerosol Generation

Two methods of aerosol generation were developed during the course of this study. The first consisted of simply passing nitrogen through a  $H_2SO_4$  saturator and into the cooled reaction cell. This produced homogeneous nucleation of  $H_2SO_4$  particles in the cell. The second technique, used to provide a better characterized source of aerosols, consisted of utilizing an Environmental Research Corporation model 7330 Fluid Atomization Aerosol Generator in conjunction with a laminar flow cooling system designed during this study and constructed from Pyrex glass.

The ERC aerosol generator consists of an atomizer aerosol source with an impactor section to remove particles with diameters larger than 0.5 microns. The impactor is followed by a beta radiation source to remove any static charge from the particles. The output from this generator was passed directly into the laminar flow cooling system shown in Figure 3. The laminar flow system was designed to pre-cool the aerosols before they entered the reaction chamber to improve the stability of the aerosol size distributions and concentrations during the flow experiments. The transport-cooling system consists of three sections, the aerosol inlet tube, a water warming jacket around the inlet tube, and a cold nitrogen sheathing flow tube around the outside. The effect of this flow arrangement is to keep the aerosol particles entrained in the center of the flow tube to prevent their colliding with a surface, while cooling of the particles is produced by contact with the liquid nitrogen boil off sheathing flow.

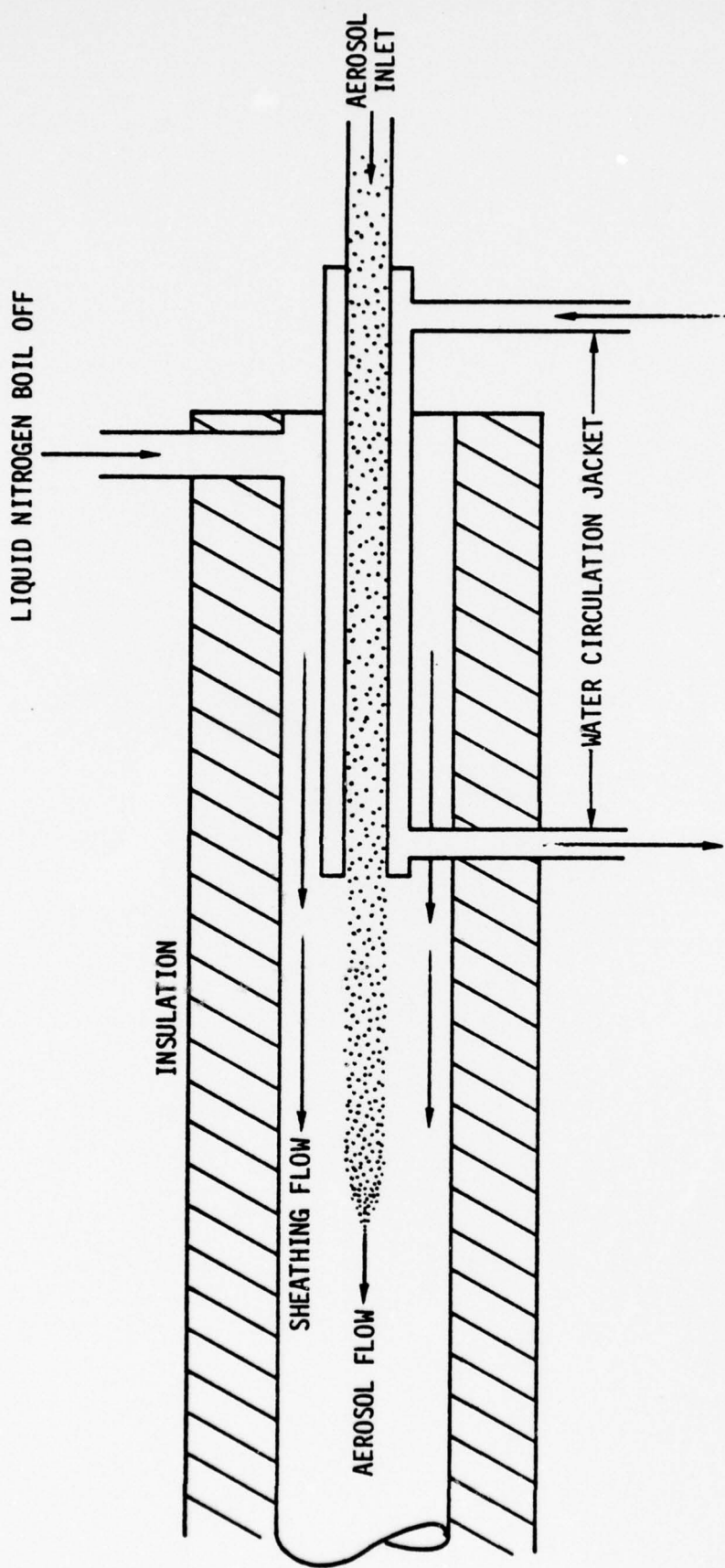


Figure 3. Schematic Diagram of Sheathed Flow Aerosol Precooling System

The size distributions and concentrations of the aerosols formed during the experiments were determined by a Thermo System Electrical Aerosol Analyzer Model 3030. This instrument measures the number concentration of aerosol particles in specific size increments in situ, by drawing a continuous sample of particles into a steady flow system, charging the aerosol particles to an electrical mobility which is a function of particle size and then measuring the mobility distribution of the aerosol particles. A detailed description of the instrument has been presented by Liu (5). From the number density and size distribution a surface area could be calculated for the particles, assuming them to be spherical.

#### Reactant Preparation

The sulfuric acid used in the experiments was reagent grade, fuming  $H_2SO_4$ . The nitrogen was Matheson Ultra-high Purity, and the oxygen was 99.6% purity, further purified by passage through a Matheson water removal filter and a liquid argon cold trap. All gas flows were measured by Hastings Mass Flowmeters.

The ozone for the experiments was produced by the use of a plasma discharge through oxygen. The discharge unit consisted of two concentric glass tubes separated by a 2 mm clearance. The center tube was filled with a concentrated solution of  $CuSO_4$  in dilute sulfuric acid in which one lead from a 12,000 volt AC transformer was submerged. The other lead was attached to copper foil wrapped around the outer tube. When the transformer bias was applied across the gap between the tubes with oxygen flowing through the gap, a plasma was generated which produced ozone from the reaction of oxygen atoms with molecular oxygen. Through the use of this generator stable flows of ozone could be produced at levels of up to 15% of the total oxygen flow. Ozone concentration in the reaction chamber could be monitored either by its infrared absorption at 9.6 microns, or by using an REM chemiluminescence ozone monitor.

#### Experimental Procedure

In the course of the program three types of experiments were conducted. These consisted of aerosol generation, aerosol plus ozone flow and static cell experiments with ozone exposed to known surface areas of sulfuric acid, and sulfuric acid diluted in water.

The aerosol generation experiments consisted of investigating various flow rates, inlet port configurations, and sample analysis procedures to maxi-

mize the surface area of the particles and to attain a steady-state condition within the reactor over the temperature range from 217 - 263K.

The flow experiments consisted of mixing ozone with the steady-state aerosol flow to observe the heterogeneous reaction rate. In these experiments the reaction chamber was cooled to a stable temperature, then "conditioned" with the sulfuric acid aerosol flow and ozone for two hours, then the aerosol generator was turned off, and a steady-state ozone concentration established for a fixed set of flow rates. The ozone concentration was determined and then the aerosol flow was re-established. When steady-state was again reached, the ozone concentration was determined along with the aerosol number concentration and size distribution. The steady-state flow equations were used for data analysis and will be described in the Results section of this report.

The third type of experiments conducted during this program were static cell measurements of ozone decay with a known surface area of sulfuric acid or sulfuric acid and water present in the cell. In these experiments the cell was first conditioned with both sulfuric acid vapor and ozone at the desired temperature and then background ozone decay measurements were made by filling the cell with  $O_3$  in either oxygen or a 80% nitrogen- 20% oxygen mix carrier gas. The ozone concentration was monitored as a function of time by infrared spectroscopy to observe its decay rate in the chamber. Upon completion of the background decay measurements, the cell was warmed to room temperature, and a known surface area of sulfuric acid or sulfuric acid and water was placed in the cell in Petri dishes, supported in the center of the reaction chamber on a stainless steel mesh. The chamber was cooled down again and re-filled with the same ozone-carrier gas mixture as in the background run. Again the ozone disappearance was monitored as a function of time. The difference between the decay rate of ozone in the two experiments was attributed to the presence of the bulk acid in the chamber. The sulfuric acid surface was renewed after each experiment to avoid the buildup of products or contaminants.

In order to determine the dependence of the heterogeneous reaction rate upon the experimental parameters, series of experiments were conducted in which the ozone concentration, sulfuric acid surface area, and relative humidity of the system were varied.

### 3.0 DATA ANALYSIS AND RESULTS

The initial experiments conducted in this study were calibration runs to verify the experimental techniques being used. These experiments include detector calibrations, ozone concentration determinations, and frozen water and sulfuric acid aerosol generation to align the aerosol flow system.

#### Gas Analysis Calibration

The spectroscopic calibrations consisted of verifying that Beer's law applied to ozone for the concentrations which were being utilized in the reactions, and determining the calibration of the reference detector against the HgCdTe detector to provide an accurate measurement of the background signal intensity. The calibrations showed that the reference detector supplied a measurement of the actual Nernst glower output intensity at 9.6 microns with an accuracy of  $\pm 0.5\%$ . Beer's law was verified for ozone by performing successive dilutions on fixed concentrations of ozone in the reaction cell. These measurements showed the optical density to be linear in ozone concentration for values of  $\ln (I_0/I)$  less than 0.7, with an accuracy of  $\pm 0.005$ . In order to obtain the best accuracy in the spectroscopic ozone measurements optical densities of about 0.5 were routinely used, corresponding to ozone concentrations on the order of  $5 \times 10^{17}$  molecules/cm<sup>3</sup>.

When the chemiluminescent ozone monitor was utilized to monitor the ozone in the reaction chamber O<sub>3</sub> concentrations of  $10^{13} - 10^{14}$  molecules/cm<sup>3</sup> were normally used. The REM chemiluminescent O<sub>3</sub> monitor was calibrated against a U.V. Products SOG standard ozone source. The REM monitor was connected to the flow stream from the reaction chamber through a total particle filter made of Gelman Spectro Grade A glass fiber. This filter removed the H<sub>2</sub>SO<sub>4</sub> particles from the flow stream to protect the REM monitor.

#### Aerosol Generation

The initial aerosol flow experiments were conducted with water particles from the ERC Fluid Atomizer. These experiments produced considerable condensation of liquid water in the chamber, showing the need for precooling of the aerosols to assure that the particles were at the desired reaction temperature. In order to precool the particles they were passed from the aerosol generator into the sheathed flow cooling system described in the Experimental Section.

The liquid nitrogen boil off vapor in this flow tube served as a sheathing flow to cool the aerosols while not impacting them on the tube walls. With this flow arrangement pre-frozen water particles were produced at stratospheric temperatures and passed into the reaction chamber.

These ice particles were then used to define the flow conditions under which the sulfuric acid particle experiments were to be run. By moving the aerosol analysis probe through the reaction chamber and using various flow rates the conditions for most stable aerosol concentrations and size distribution could be determined. Figures 4 & 5 show some typical data taken by the Electrical Aerosol Analyzer for water aerosols flowing through the system at 253K with sampling point set 30 cm from the back of the chamber. The water aerosols were primarily small particles with the maximum number concentration occurring at a mean diameter of 0.025 microns. This size distribution can be used to calculate a total volume and surface area for the assumed spherical particles as shown in Table 1, by summing the mean volume and area values calculated for the number of particles observed in each size range. These data were collected for a flow rate of 4.25 liters/minute giving a half-life for the particles in the cell of 5.2 minutes. These flow rates were found to produce stable conditions within the cell, where the total surface area of the particles entering the cell differed by less than 13% from that of the particles at the exit port.

TABLE 1.  $H_2O$  AEROSOL AT 253K

$\Sigma N (> 0.01 \mu m)$ (number/cm <sup>3</sup> )	$\Sigma S$ ( $\mu m^2/cm^3$ )	$\Sigma V$ ( $\mu m^3/cm^3$ )
$2.15 \times 10^5$	$5.76 \times 10^2$	4.81

MEAN DIAMETER OF MAXIMUM SURFACE AREA = 0.04  $\mu m$

TOTAL CELL VOLUME = 22.25 l

TOTAL PARTICLE SURFACE AREA = 0.13  $cm^2$

TOTAL PARTICLE VOLUME =  $1.06 \times 10^{-7} cm^3$

FLOW RATE: 4.25l/min.

CELL HALFLIFE = 5.2 minutes

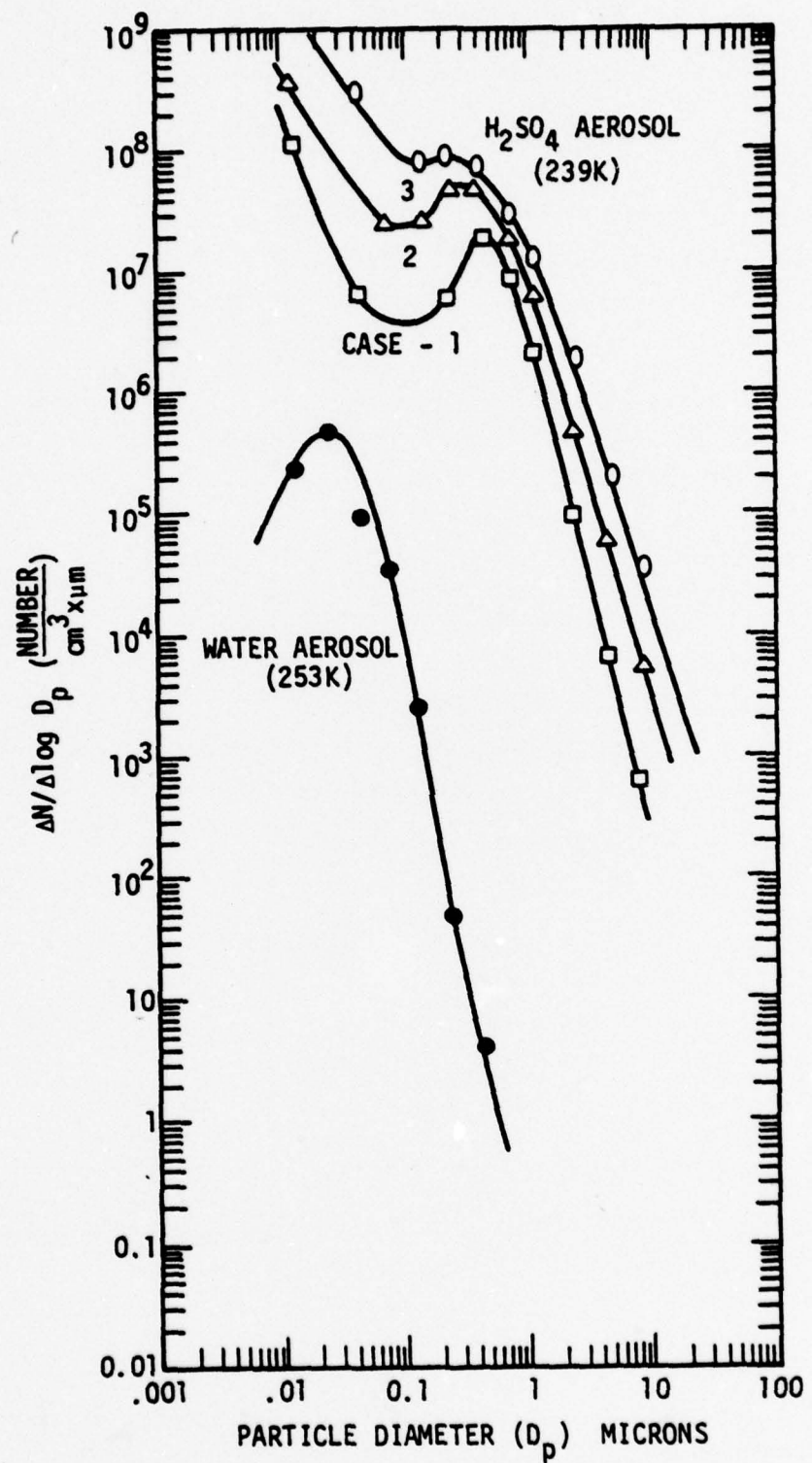


Figure 4. Log-normal Plot of Number Concentration of  $\text{H}_2\text{O}$  and  $\text{H}_2\text{SO}_4$  Aerosols Generated in Flow Experiments.  
The Experimental Conditions are Given in Tables 1 & 2.

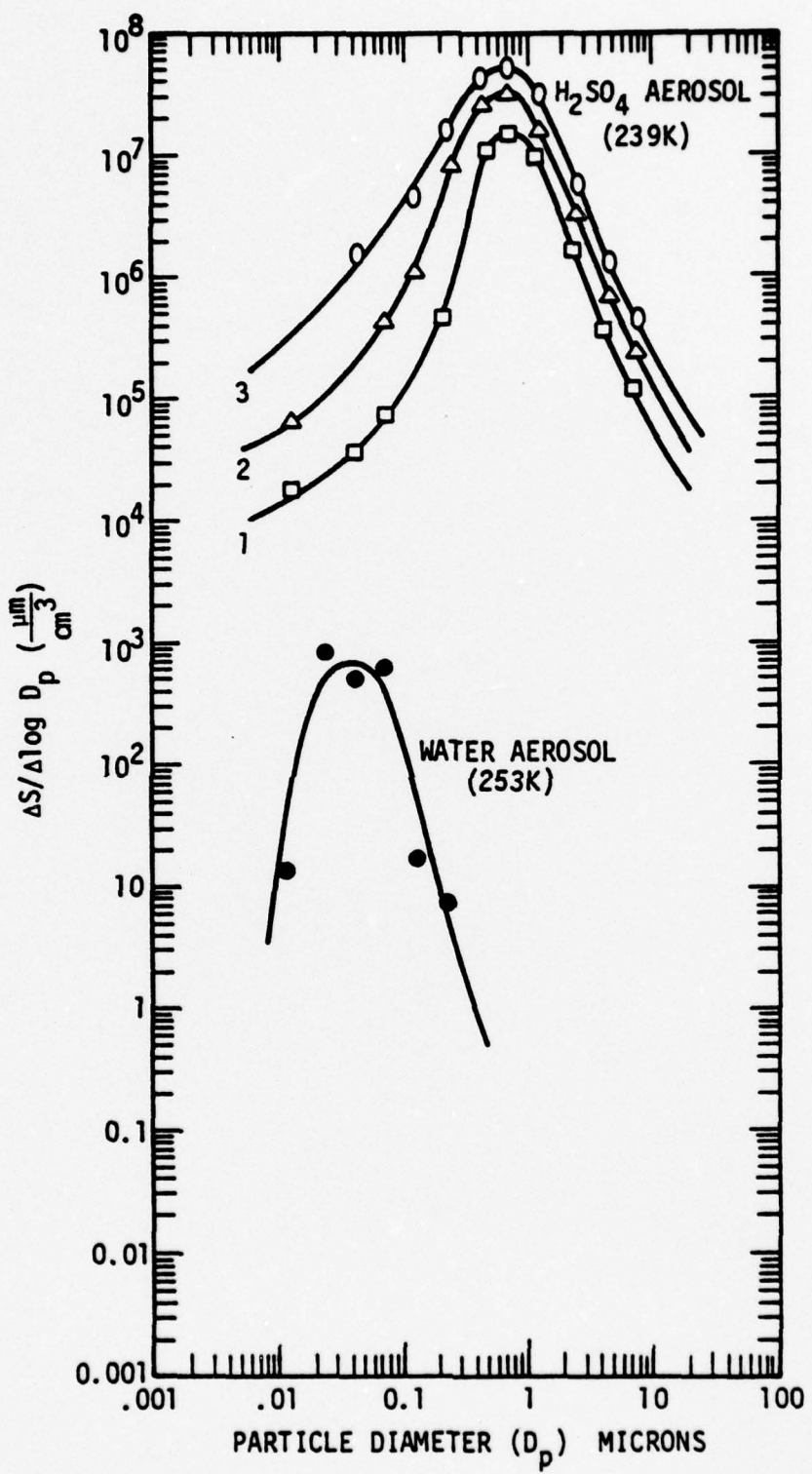


Figure 5. Log-normal Plot of Surface Area Concentration of  $\text{H}_2\text{O}$  and  $\text{H}_2\text{SO}_4$  Aerosols Generated in Flow Experiments. The Experimental Conditions are given in Table 1 & 2.

Based upon the results of the water aerosol generation experiments, studies were carried out using fuming sulfuric acid to generate aerosols at reduced temperatures. The initial sulfuric acid aerosol generation experiments were designed to observe the extent to which nucleation of the cooled sulfuric acid vapor would affect the experimental results. This was accomplished by using a room temperature  $H_2SO_4$  saturator to pass acid vapor into the chamber through the laminar flow cooling tube. These experiments demonstrated that there was sufficient super-saturation of  $H_2SO_4$  vapor and adequate  $H_2O$  present (approximately 10 ppm in the carrier gases) that abundant small aerosol particles were formed by homogeneous and binary nucleation of sulfuric acid and sulfuric acid and water. Since nucleation and growth of the particles would cause a changing surface area within the reaction chamber, it was found preferable to use the fluid atomization technique to generate larger particles to obtain a more stable aerosol surface area.

Figures 4 and 5 also show the aerosol data for a series of particle generation experiments conducted with fuming  $H_2SO_4$  in the ERC aerosol generator, and graphed using a log normal distribution. The Electrical Aerosol Analyzer was used to describe the sub-micron particles, with the larger particles being characterized by a Climet Optical Particle Counter. The data are for three runs conducted at different flow rates. In each case a bi-modal size distribution was produced by the combination of the agglomeration of the atomized aerosol material in the introduction flow tube and the formation of new small particles by nucleation. The surface area of the aerosols was primarily associated with the larger particles, and increased with flow rate through the aerosol generator as shown in Table 2. The particle size distributions and surface area remained fairly constant in the reaction chamber for flow rates between 3 and 6 litres/min as observed by moving the sampling probe through the cell. Hence the half-life of the particles in the cell was set at about 5 1/2 minutes for the subsequent runs.

TABLE 2.  $H_2SO_4$  AEROSOLS AT 239K

	Flow Rate ( $\text{L}/\text{min}$ )	$\Sigma N (> 0.01 \mu\text{m})$ (number/ $\text{cm}^3$ )	$\Sigma S$ ( $\mu\text{m}^2/\text{cm}^3$ )	$\Sigma V$ ( $\mu\text{m}^3/\text{cm}^3$ )
1.	2.83	$5.44 \times 10^7$	$1.11 \times 10^7$	$1.60 \times 10^6$
2.	3.78	$1.78 \times 10^8$	$2.4 \times 10^7$	$3.28 \times 10^6$
3.	4.25	$1.92 \times 10^8$	$3.84 \times 10^7$	$4.8 \times 10^6$
		Case 1	Case 2	Case 3
Total Surface area ( $\text{cm}^2$ )		2240	5280	8450
Total Volume ( $\text{cm}^3$ )		0.035	0.072	0.11
Flow Rate $\text{L}/\text{min}$	2.83	3.78	4.25	
Cell Half Life (min)	7.2	5.8	5.2	

Having established the capability of generating reproducible levels of  $H_2SO_4$  aerosols, flow experiments with mixtures of aerosols and ozone were conducted using the steady-state flow kinetics technique. This technique is based upon balancing the rate of decomposition of a reactant by the flow of fresh materials into the reaction chamber. The first order decay rate constant of ozone in the reaction chamber, for a fixed surface area of aerosol particles is given by

$$k_{\text{decay}} = k_{H_2SO_4} - k_{\text{walls}} = \ln(2)/T_{1/2} \quad (1)$$

where  $T_{1/2}$  is the ozone decay half life observed in the chamber and  $k_{\text{walls}}$  and  $k_{H_2SO_4}$  are the first order heterogeneous decay rate constants of  $O_3$  on the chamber walls and  $H_2SO_4$  particles respectively with units of  $\text{sec}^{-1}$ . In the steady-state flow system with good reactant mixing  $k_{\text{decay}}$  can be experimentally determined from the expression

$$k_{\text{decay}} = \frac{\text{FLOW RATE}}{\text{CELL VOLUME}} \left\{ \frac{[O_3]_{\text{in}} - [O_3]_{\text{ss}}}{[O_3]_{\text{ss}}} \right\}, \quad (2)$$

and  $k_{H_2SO_4}$  can be obtained from equation (1) by measuring the wall decay rate constant in the absence of acid aerosols.

The sensitivity of the steady-state flow technique is limited by the residence time and concentrations of the reactants in the chamber. Since as shown in Table 2 the flow rate and aerosol concentrations were directly re-

lated in these experiments, the sensitivity of the method was essentially limited by the ability of the gas analysis technique to determine significant differences between the  $O_3$  concentrations with and without the presence of the aerosol particles. In the flow experiments the REM chemiluminescence  $O_3$  monitor was used and it had sufficient sensitivity to determine a 5% change in the  $O_3$  concentration. Based upon the flow rates of Case 2 in Table 2 and the cell volume of 22.25 liters, equation (2) shows that an observed 5% change in the  $O_3$  concentration within the reaction chamber corresponded to a heterogeneous decomposition rate constant for  $O_3$  on  $H_2SO_4$  of  $k_{H_2SO_4} = 1 \times 10^{-2} \text{ (sec}^{-1}\text{)}$ . For the total aerosol surface area of  $2.4 \times 10^7 \mu\text{m}^2/\text{cm}^3$  observed in Case 2, the method had the sensitivity to observe a reaction efficiency of  $\geq 1.6 \times 10^{-6}$  reactions per gas-surface collision at 239K based upon the gas kinetic expression

$$\gamma = \left\{ \frac{1}{4} \left( \frac{8}{\pi} \frac{RT}{M} \right)^{\frac{1}{2}} [\text{Surface Area } H_2SO_4] \right\}^{-1} k_{H_2SO_4} \quad (3)$$

where R is the gas constant, T the absolute temperature, and M the molecular weight of the reacting gas. However even with this sensitivity no reproducible variation in the ozone steady-state concentration in the reaction chamber was observable upon the introduction of the  $H_2SO_4$  aerosols under the conditions described in Table 2.

The inability of the  $H_2SO_4$  aerosols to produce an observable change in the  $O_3$  concentration in the chamber in the time scale of the reaction demonstrated that the reaction efficiency of the heterogeneous decomposition of  $O_3$  was less than or equal to  $10^{-6}$  reactions per gas-surface collision. With this low an efficiency it is doubtful that the reaction of ozone with pure  $H_2SO_4$  particles is of significance in stratospheric chemistry, however it was still desirable to investigate the heterogeneous decomposition of ozone to provide insight into the fundamental mechanisms of this class of reactions. To obtain the sensitivity required to determine the dependence of the decomposition reaction upon temperature and reactant concentration, a series of static cell experiments were conducted using a calibrated surface area of  $H_2SO_4$  placed in the reaction chamber in Petri dishes.

The basic method for the static cell experiments was outlined in the Experimental Section of this report. In these experiments the cell was cleaned thoroughly, purged to remove water, then conditioned with  $H_2SO_4$  vapor and  $O_3$  before any kinetic measurements were made. After the conditioning

process the cell was calibrated for the wall decay rate of  $O_3$  in the absence of the  $H_2SO_4$  containers by observing the  $O_3$  infrared absorption at 9.6 microns and then the measurements were repeated in the presence of the calibrated surface area of fuming  $H_2SO_4$  or  $H_2SO_4 - H_2O$  mixture. The rate measurements were made over the temperature range from 217 - 263K at one atmosphere of oxygen or a 80/20 nitrogen-oxygen mix. The half life of the ozone in the cell due to the presence of the measured surface of  $H_2SO_4$  was determined and  $k_{H_2SO_4}$  calculated from equation (1). This value was then used in equation (3) to obtain the reaction efficiency.

Utilizing this technique, experimental conditions were varied to determine the reaction dependence upon ozone concentration and  $H_2SO_4$  surface area. Figure 6 shows the natural logarithm of the optical density of the ozone IR absorption versus time for a series of experiments at 235K in which the data have been normalized to an initial optical density for  $O_3$  absorption of 0.4 and a  $H_2SO_4$  surface area of  $103.3 \text{ cm}^2$ . The linearity of the data indicate that the heterogeneous decay process was indeed first order with respect to the  $O_2$  concentration and the acid surface area.

The temperature and M gas dependence of the reaction efficiency are shown in Figure 7 for both the fuming  $H_2SO_4$  surface and a mixture of 10% by volume  $H_2SO_4$  in distilled  $H_2O$ . In this figure the negative logarithm of  $\gamma$  is plotted versus  $1/T$  with the experiments using oxygen as the carrier gas indicated by triangles and those in 80/20 nitrogen-oxygen shown in open circles. The good correspondence between the data points for the two carrier gas systems indicates that the surface reaction does not involve gaseous oxygen. Also the linearity of the plots indicates that the reaction rate is controlled by the kinetic temperature of the gaseous molecules. The data point above 263K shows a significantly higher efficiency than those at lower temperatures, which is attributed to the  $H_2SO_4$  being a super cooled liquid at this temperature, and a frozen solid at lower temperatures.

Judeikis and Siegel (6) have derived a simplified kinetic model to describe heterogeneous gas-surface reactions based upon kinetic gas theory and the transition state model of reaction kinetics. Their derivation shows that the reaction efficiency should have a temperature dependence given by a relationship of the following form:

$$\gamma = A(1 + B \exp[(E_p - E_a)/RT])^{-1} \quad (4)$$

In this expression A is a constant determined by the sticking coefficient for

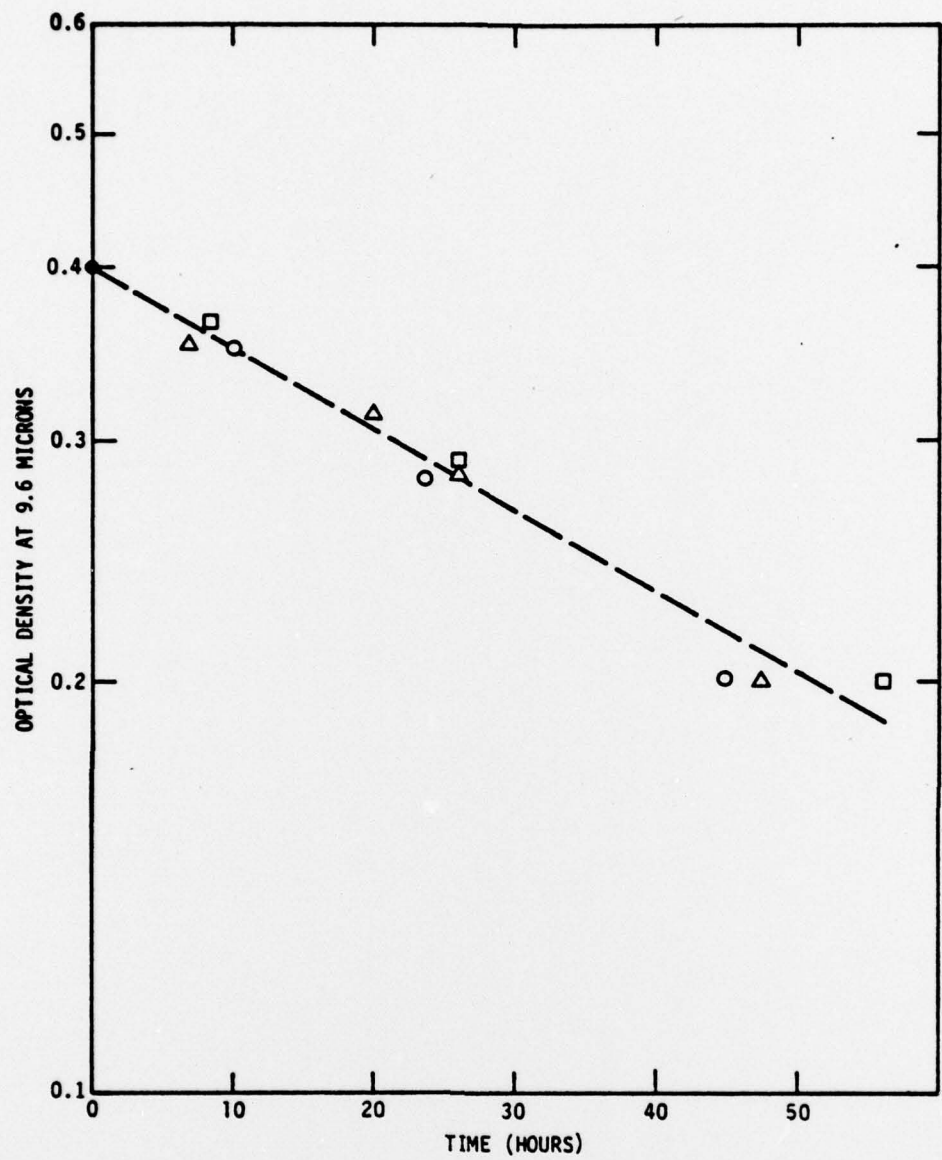


Figure 6. Semi-logarithmic plot of the optical density of the 9.6 micron ozone optical density versus time for three static cell reaction experiments. The data have been normalized to the same initial optical density of ozone and to the same surface area of  $\text{H}_2\text{SO}_4$ . Initial conditions

	Optical Density	$\text{H}_2\text{SO}_4$ Surface Area (cm <sup>2</sup> )
□	.525	103.3
△	.423	103.3
○	.675	49.5

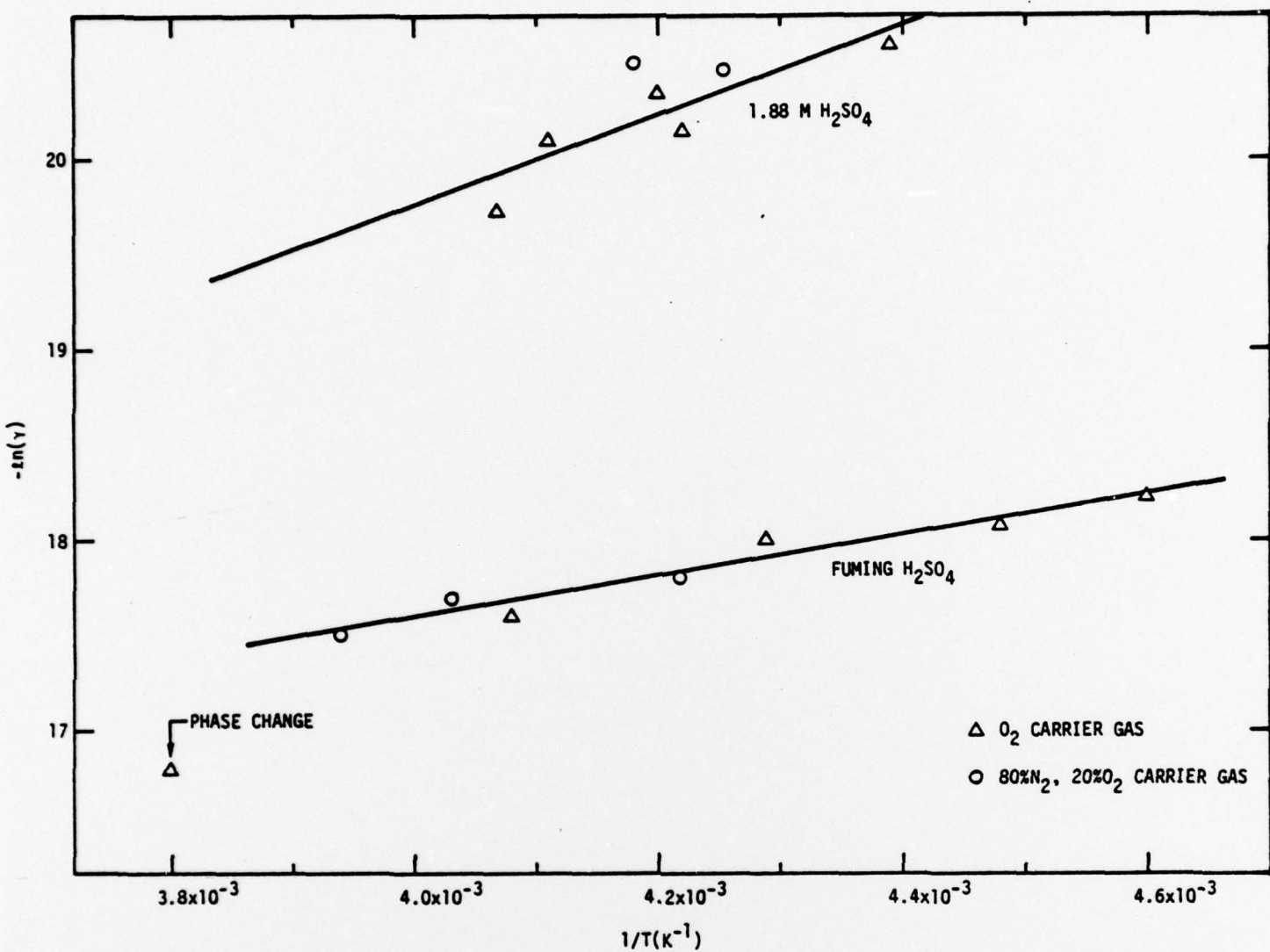


Figure 7. Semi-logarithmic Plot of the Measured Reaction Efficiency (reactions / collision) of the Ozone Decomposition Versus Reciprocal Absolute Temperature for Fuming  $H_2SO_4$  and Dilute  $H_2SO_4$  in  $H_2O$ .

adsorption onto the reaction surface, and the number of available reaction sites on the reactive surface. The constant B is a ratio of the partition functions of the activated surface complex and the gas phase species and is a measure of the mobility of the activated complex on the surfaces.  $E_r$  is the activation energy of the overall chemical reaction, while  $E_a$  is that part of the experimental activation energy associated with the adsorption of the reacting gas on the surface.

To get an empirical estimate of the magnitudes of A and B, the plot of the natural logarithm of  $\gamma$  versus  $1/T$  was examined. As shown in Figure 7 this plot for the case of fuming  $H_2SO_4$  is quite linear for temperatures below 260K where the  $H_2SO_4$  changes phase to become a solid from the super-cooled liquid. The linearity of the plot suggests that in this case the  $O_3$  is quite mobile on the  $H_2SO_4$  surface and that  $B > A$ . Under these conditions equation (4) simplifies to the form,

$$\gamma = [AB \exp(E_r - E_a)/RT]^{-1} \quad \text{for } T \text{ less than } 260K \quad (5)$$

Using this empirical form to describe the data, the constants can be evaluated to give:

$$\gamma = [5.85 \times 10^5 \exp(1081/T)]^{-1} \quad \text{for solid fuming } H_2SO_4 \text{ at } T < 260K$$

The values for  $\gamma$  from this expression have an experimental uncertainty of about  $\pm 10\%$  over the temperature region covered. The data for the 1.88 M  $H_2SO_4$  in  $H_2O$  cover a smaller temperature range and show more scatter, yet they do show a monotonic increase in  $\gamma$  with temperature and can be described by equation (5). Evaluating the constants from Figure 7 gives

$$\gamma = [3.06 \times 10^4 \exp(2360/T)]^{-1} \quad (7)$$

for frozen 1.88 M  $H_2SO_4$  at temperatures between 228 - 246K with an experimental uncertainty of  $\pm 30\%$ .

These reaction efficiency data have had the background rate constant for ozone decay on the chamber walls subtracted out through equation (1). The decay half-life of the ozone on the reaction chamber conditioned with fuming  $H_2SO_4$  and  $O_3$  at 237K was 71.4 hours, while the half-life attributable to the measured  $H_2SO_4$  surface was 139 hours. In the case of the 1.88 M  $H_2SO_4$

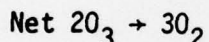
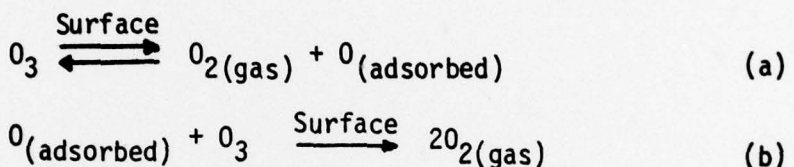
the background decay half-life at 237K was measured to be 1,428 hours, with that attributed to the measured acid surface area being 408 hours. The large difference in these background decay rates was due to the higher vapor pressure of  $H_2SO_4$  in the studies with the fuming acid providing a greater surface area of acid condensing out on the chamber walls. In both sets of experiments the background data was reproducible and did not present any experimental difficulties to measure.

#### 4.0 DISCUSSION

The technique for generation of sulfuric acid aerosols in a flow system at stratospheric temperatures developed during this study has been shown capable of producing stable aerosol surface area concentrations large enough to allow heterogeneous reaction efficiencies on the order of  $10^{-6}$  reactions/collision to be measured. The flow reactor experiments demonstrated that total surface area concentrations of up to  $4 \times 10^7 \mu\text{m}^2/\text{cm}^3$  of acid aerosol particles could be generated at stratospheric temperatures in a reaction chamber, and that this surface area concentration could be maintained in a stable fashion for cell half-lives on the order of 5 to 10 minutes. The major experimental requirements for maintaining this level of particles were found to be humidity control, aerosol generation by atomization, and sheathed air precooling of the aerosol particles. This surface area concentration coupled with sensitive gas analysis methods gives the steady-state flow kinetics technique a sensitivity that can be matched by static cell measurements only by using high volume cells with large areas of bulk material or by running reactions from 20 to 100 times longer than required in the flow system. This technique also offers the ability to experimentally determine if the physical and chemical surface properties of aerosol particles do produce significant differences in heterogeneous reaction rates when compared to bulk material surfaces.

The heterogeneous reactions of ozone on  $\text{H}_2\text{SO}_4$  and  $\text{H}_2\text{SO}_4 + \text{H}_2\text{O}$  studied in this program were found to have reaction efficiencies of less than  $10^{-6}$  reactions/collision in the aerosol flow studies. Hence these reaction systems did not provide an opportunity to carry out detailed analysis by the steady-state flow technique. In order to provide the necessary temperature dependence and mechanistic data, static chamber experiments were carried out which showed the actual reaction efficiencies to be on the order of  $10^{-8}$  and  $10^{-9}$  respectively at stratospheric temperatures. The slowness of the  $\text{O}_3$  heterogeneous decomposition on  $\text{H}_2\text{SO}_4$  is not surprising since sulfuric acid is considered a poor catalyst in general. Though  $\text{H}_2\text{SO}_4$  is postulated to make up the bulk of the stratospheric aerosols, it has been suggested that the impurities in the sulfuric acid aerosols (metallic cations, silicates, soil particles, carbon soot, etc.) would be the major reactive components. In order to study the heterogeneous reactions of impure  $\text{H}_2\text{SO}_4$  aerosols, however it is required that the reactions in the pure system be understood.

The experimental data show that the decomposition of ozone on the sulfuric acid surfaces is a first order process with respect to both  $O_3$  concentration and acid surface area, and that the reaction is independent of the gas phase concentration of molecular oxygen. It is also apparent from the total number of  $O_3$  molecules removed by the available acid surface area that the reaction is a catalytic decomposition rather than simple adsorption. In a typical run, over  $10^{21}$  ozone molecules were decomposed on an acid surface area of only  $10^{18} \text{ \AA}^2$ . For simple adsorption this would correspond to  $10^3$  to  $10^4$  monolayers of ozone build up on the acid surface which is unlikely. A possible catalytic decomposition mechanism would be via



This mechanism has ozone decomposing on a surface to yield gaseous  $O_2$  and an adsorbed oxygen atom which can then react with a second  $O_3$  molecule on the surface to form two more oxygen molecules. To reconcile this two step mechanism with the agreement of the measured reaction efficiencies with Judeikis and Siegel's transition-state theory (equation (4)) would require that one of the above reactions be a rate determining step. Since (a) involves breaking a bond and forming an adsorbed species it is quite possible that its rate could be considerably slower than that of (b). The large value obtained for the constant B in equation (4), the ratio of the partition functions of the activated surface complex (minus one degree of freedom leading to dissociation) and the adsorbed gas molecule, indicates that ozone forms a very mobile complex on the surface which is not bound to a specific surface site. Also the small values obtained for  $(E_r - E_a)$  indicate that the activation energy for adsorption of the ozone is only about 1 Kcal/mole less than the activation energy required for the overall dissociation. Such a mobile surface complex whose formation activation energy is close to that required for dissociation could be the intermediate in the observed catalytic ozone decomposition.

The water content of stratospheric aerosols must be estimated to assess the significance of the observed decrease in catalytic efficiency of the  $H_2SO_4$

surface with water dilution. This is difficult as the water content is a function of both the relative humidity and  $H_2SO_4$  particle size. However from the calculations of Mirbel and Katz (7), it can be estimated that due to the low relative humidity, stratospheric aerosols contain less than 50% mole fraction  $H_2O$ . Since the 0.045 mole fraction of  $H_2SO_4$  in  $H_2O$  used in these experiments produced only a factor of 10 decrease in the reaction efficiency, it is unlikely that the  $H_2O$  in actual stratospheric aerosols has any great effect upon  $H_2SO_4$  heterogeneous reaction rates.

## 5.0 RECOMMENDATIONS FOR FUTURE RESEARCH

To provide the information required to make an assessment of the importance of heterogeneous reactions in stratospheric chemistry, research in several areas is required. The effects of metal oxide, carbon, silicate and halide impurities in  $H_2SO_4$  particles upon heterogeneous reaction efficiencies must be determined, and the possible photochemical enhancement of reaction rates by solar radiation should be investigated. There is substantial evidence that the impurities in the stratospheric aerosol particles may have much higher catalytic efficiencies than those observed for pure  $H_2SO_4$  in this study. Cadle et al. (3) report recalculations of data from Aldaz (8) and Kroening and Ney (9) giving values of  $\gamma = 3 \times 10^{-6}$  and  $\gamma = 2 \times 10^{-4}$  for the decomposition of  $O_3$  on soil and black rubber respectively, while the work of Novakov, Chang, and Harker (10) and Chang and Novakov (11) has demonstrated the reactive properties of carbonaceous particles toward both  $SO_x$  and  $NO_x$  gases. These studies and the well known catalytic properties of the transition metal oxides make it imperative that the effect of these impurities upon the heterogeneous reaction rates of stratospheric aerosols be determined.

The photochemical effects of solar irradiation of particle surfaces in the presence of the reactive stratospheric gases is also an unanswered question. It is known the transition metal oxide surfaces can act as photosensitizing agents for a number of chemical reactions including liquid phase reactions such as the formation of hydrogen peroxide,  $H_2O_2$ , from water and oxygen in a photosensitized surface reaction. (12) The abundance of shorter wavelength solar radiation in the stratosphere also enhances the possibility of the importance of such photosensitized heterogeneous reactions.

There are a number of heterogeneous reaction systems which require experimental study with a few of those which have a greater potential for importance in the stratosphere being:

- 1) Reactions of  $N_2O_5$  with surface  $H_2O$  to produce  $HNO_3$ .
- 2) The oxidation of  $NO_x$ ,  $SO_x$ , and  $ClO_x$  species by photosensitized metal oxide surfaces and by adsorbed  $H_2O_2$ .
- 3) The catalytic decomposition of ozone and  $ClNO_3$  on impure  $H_2SO_4$  aerosols with and without solar irradiation.
- 4) The recombination of atomic species on aerosol surfaces. Akers and Wrightman report  $O + O \rightarrow O_2$  occurs on  $H_2SO_4$  with an efficiency of  $\gamma = 5 \times 10^{-5}$  (13).

In addition to investigating these classes of reactions it would be very desirable to conduct parallel studies on a single reaction system using both an aerosol particle flow system and a bulk surface system to obtain comparison data. The question of the validity of using a bulk surface to represent aerosol surfaces is a key one for the assessment of much of the current ongoing experimental work. The surface geometry and crystalline structure of submicron super-cooled or frozen particles could be substantially different from that of bulk material, and small particles are also subject to charging phenomena in the atmosphere which bulk surfaces cannot represent. The number of reactive sites may be substantially different in actual aerosol particles, and this possibility should be investigated before a mass of bulk surface data is collected and used to represent the heterogeneous reactivities of particles in the atmosphere.

Some of these questions will be addressed in continuing studies in this laboratory specifically the role of impure surfaces as photosensitization sites, and the problem of comparing bulk surface properties to those of aerosol particles. The initial reaction system to be investigated will include the decomposition of ozone on  $H_2SO_4$  aerosols containing Al, V, and Fe oxides with and without irradiation and the generation of  $HNO_3$  from  $N_2O_5$  on 50/50  $H_2SO_4/H_2O$  particles.

#### REFERENCES

- 1) "Environmental Impact of Stratospheric Flight", National Academy of Sciences, Washington, D. C. (1975).
- 2) "The Stratosphere Perturbed by Propulsion Effluents", CIAP Monograph 3, Department of Transportation Report DOT-TST-75-53, pp. 6-1 - 6-63, (1975).
- 3) Cadle, R. D., Crutzen, P. and Ehhalt, P., "Heterogeneous Chemical Reactions in the Stratosphere", Journal of Geophysical Research 80, pp. 3381-3385, (1975).
- 4) Judeikis, H. S., "Heterogeneous Reactions in the Stratosphere", presented at the 2nd International Conference on the Environmental Impact of Aerospace Operations in the High Atmosphere, AMS/AIAA, July 8-10, 1974, San Diego, California.
- 5) Liu, B.Y.H., Whitby, K.T. and Pui, P.Y.H., "A Portable Electrical Analyzer for Size Distribution Measurements of Submicron Aerosols", Journal of the Air Pollution Control Association 24, pp. 1067-1072 (1974).
- 6) Judeikis, H. S. and Siegel, S., "Particle-Catalyzed Oxidation of Atmospheric Pollutants", Atmospheric Environment 7, pp. 619-631 (1973).
- 7) Mirabel, P. and Katz, J. L., "Binary Homogeneous Nucleation As a Mechanism For The Formation of Aerosols", Journal of Chemical Physics 60, pp. 1138-1145 (1974).
- 8) Aldaz, L., "Flux Measurements of Atmospheric Ozone Over Land and Water", Journal of Geophysical Research 74, pp. 6943-6946 (1969).
- 9) Kroening, J. L. and Ney, E. P., "Atmospheric Ozone", Journal of Geophysical Research 67, pp. 1867-1875 (1962).
- 10) Novakov, T., Chang, S. G., and Harker, A. B., "Sulfates as Pollution Particulates: Catalytic Formation on Carbon (SOOT) Particles", Science 186, pp. 259-261 (1974).
- 11) Chang, S. G. and Novakov, T., "Formation of Pollution Particulate Nitrogen Compounds by NO-SOOT and NH<sub>3</sub>SOOT Gas-Particle Surface Reactions", Atmospheric Environment 9, pp. 495-504 (1975).
- 12) Calvert, J. G., Theurer, K., Rankin, G. T., and MacNevin, W. M.; Journal American Chemical Society 76, p. 2575 (1954).